Oriented Bioconjugation of Unmodified Antibodies to Quantum Dots Capped with Copolymeric Ligands As Versatile Cellular Imaging Tools

ARTICLE *in* ACS APPLIED MATERIALS & INTERFACES · NOVEMBER 2015

Impact Factor: 6.72 · DOI: 10.1021/acsami.5b09777

11 AUTHORS, INCLUDING:

Mariana Tasso

École Supérieure de Physique et de Chimie I…

18 PUBLICATIONS **89** CITATIONS

SEE PROFILE

Emerson Giovanelli

Madrid Institute for Advanced Studies

21 PUBLICATIONS **93** CITATIONS

SEE PROFILE

François Treussart

Ecole normale supérieure de Cachan

108 PUBLICATIONS **2,502** CITATIONS

SEE PROFILE

Thomas Pons

École Supérieure de Physique et de Chimie I…

107 PUBLICATIONS **3,941** CITATIONS

SEE PROFILE

ACS APPLIED MATERIALS & INTERFACES

Research Article

www.acsami.org

Oriented Bioconjugation of Unmodified Antibodies to Quantum Dots Capped with Copolymeric Ligands as Versatile Cellular Imaging Tools

Mariana Tasso,[†] Manish K. Singh,[‡] Emerson Giovanelli,[†] Alexandra Fragola,[†] Vincent Loriette,[†] Marie Regairaz,[§] François Dautry,[§] François Treussart,[‡] Zsolt Lenkei,[∥] Nicolas Lequeux,[†] and Thomas Pons*[,†]

[†]Laboratoire de Physique et d'Étude des Matériaux, ESPCI ParisTech, PSL Research University, CNRS, Sorbonne Universités, UPMC Univ. Paris 6; LPEM, 10 rue Vauquelin, F-75231 Paris Cedex 5, France

[‡]Laboratoire Aimé Cotton, CNRS, ENS Cachan, Univ. Paris-Saclay, Bâtiment 505, Campus d'Orsay, 91405 Orsay, France

[§]Laboratoire de Biotechnologies et Pharmacologie Appliquée, CNRS, ENS Cachan, Univ. Paris-Saclay, 61, Avenue du Président Wilson, 94235 Cachan, France

[∥]Brain Plasticity Unit, PSL Research University, ESPCI ParisTech, CNRS UMR 8249, 10 rue Vauquelin, 75005 Paris, France

Supporting Information

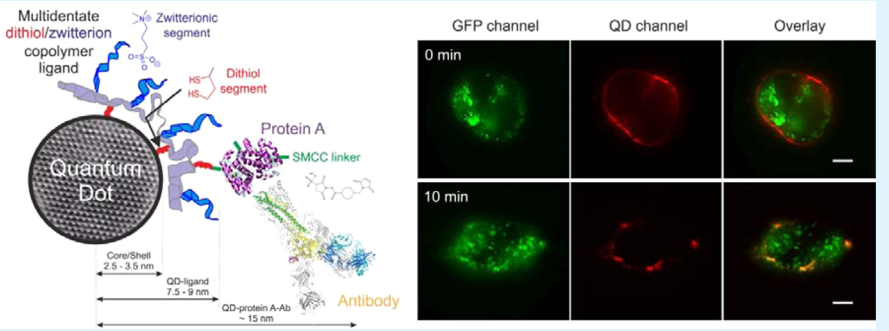

ABSTRACT: Distinctive optical properties of inorganic quantum dot (QD) nanoparticles promise highly valuable probes for fluorescence-based detection methods, particularly for in vivo diagnostics, cell phenotyping via multiple markers or single molecule tracking. However, despite high hopes, this promise has not been fully realized yet, mainly due to difficulties at producing stable, nontoxic QD bioconjugates of negligible nonspecific binding. Here, a universal platform for antibody binding to QDs is presented that builds upon the controlled functionalization of CdSe/CdS/ZnS nanoparticles capped with a multidentate dithiol/zwitterion copolymer ligand. In a change-of-paradigm approach, thiol groups are concomitantly used as anchoring and bioconjugation units to covalently bind up to 10 protein A molecules per QD while preserving their long-term colloidal stability. Protein A conjugated to QDs then enables the oriented, stoichiometrically controlled immobilization of whole, unmodified antibodies by simple incubation. This QD−protein A immobilization platform displays remarkable antibody functionality retention after binding, usually a compromised property in antibody conjugation to surfaces. Typical QD−protein A−antibody assemblies contain about three fully functional antibodies. Validation experiments show that these nanobioconjugates overcome current limitations since they retain their colloidal stability and antibody functionality over 6 months, exhibit low nonspecific interactions with live cells and have very low toxicity: after 48 h incubation with 1 μM QD bioconjugates, HeLa cells retain more than 80% of their cellular metabolism. Finally, these QD nanobioconjugates possess a high specificity for extra- and intracellular targets in live and fixed cells. The dithiol/zwitterion QD−protein A nanoconjugates have thus a latent potential to become an off-the-shelf tool destined to unresolved biological questions.

KEYWORDS: *quantum dots, oriented bioconjugation, antibodies, receptor tracking, toxicity*

1. INTRODUCTION

Water-soluble quantum dot (QD) nanoparticles have remarkable comparative advantages over organic fluorophores, the as-of-today prevalent tool in biological imaging and detection.[1,2] Biomolecules labeled with fluorophores are widely employed as cellular markers as well as in bioanalyte sensing and separation or in cell phenotyping and clinical diagnostic applications.[3−5]

Thanks to a much higher photostability, emission intensity, and

Received: October 15, 2015
Accepted: November 9, 2015

DOI: 10.1021/acsami.5b09777
ACS Appl. Mater. Interfaces XXXX, XXX, XXX−XXX

tunable, multicolored emission wavelengths, QDs constitute an attractive alternative to fluorophores and are particularly promising with regard to their potential for enhancement in detection sensitivity and in vivo medical imaging.[6−8] The applicability and utility of QDs in the inspection of biological phenomena and the detection of clinically relevant markers of disease have been vastly reported and demonstrated.[9−11] The technological transfer of these tools to the clinical and diagnostics fields remains, however, hampered by toxicity concerns and by difficulties at reproducing reported results.[1,12−14] In practice, inorganic QDs are transferred to aqueous media by a ligand exchange or encapsulation process and are thereafter functionalized with biomolecules by adopting a bioconjugation approach among the various in the palette: (1) carbodiimide chemistry,[15−18] (2) QD surface modification with avidin (streptavidin or NeutrAvidin) for the further recognition of biotin-labeled molecules,[9,18−22] (3) histidine-tagged biomolecules assembled on the QD surface via specific metal-affinity interactions,[23−26] or (4) bioconjugation of distinct ligand moieties, for example, amines, with reactive biomolecules.[27−29] A vast array of biomolecules have been immobilized on QDs from antibodies, proteins, and oligonucleotides[24,28,30−32] to any other intermediate molecule that would support the adequate immobilization of the target-recognition species.[9,10,18−22,33−36] Above all, efforts in developing efficient nanoparticle−biomolecule conjugation strategies focus on obtaining colloidally stable, non-cross-linked nanoconjugates while maintaining the full functionality of the attached biomolecule.

In the quest for effective target detection, antibodies are the prevalent candidate agents due to their commercial availability, capacity to be selected to specifically recognize a given target and high binding affinity. Antibodies (Abs) have been bound to nanoparticles either in random or in oriented conformations. Random conformations refer to bioconjugation approaches that partly or totally render the active site of the Ab inaccessible or not functional. This approach encompasses strategies where random Ab amino acids, like lysines or cysteines, are used as anchoring points to bind the Ab to the surface or to a tag or linker, like histidine or biotin.[28,37−40] Approaches of this kind typically disrupt the three-dimensional structure of whole Abs and are prone to a marked depletion in functionality.[31] A recent survey on QD bioconjugation methods found that the number and functionality of randomly bound Abs to QDs is substantially lower than the suggested estimates of 2−10 Abs per dot,[41] with 0.1 functional Ab per QD for Abs bound to the nanoparticles after Ab reduction. Oriented immobilization (OI) strategies, on the contrary, enable the surface immobilization of antibodies without jeopardizing Ab structure or function. Furthermore, OI platforms yield higher surface densities of fully functional Abs, thus maximizing the likelihood of nanoparticles' recognition of their partner molecules at the target site, a critical fact particularly in the detection of low-expression targets. The use of an Ab-binding protein, like protein A or G, as an intermediate layer on QDs[10,33−36] (or other solid[42] or nanoparticle[43] surfaces), or the site-specific modification of Abs with tags in ways that do not affect the antigen recognition site (e.g., Invitrogen SiteClick)[44] constitute examples of OI approaches. Unlike site-specific Ab modification strategies, the use of Ab-binding proteins has the advantage of requiring no Ab modification and to provide for a spacer layer between the Ab and the QD surface, thus potentially diminishing Ab denaturation.

In this work, we take advantage of our previous achievements in the surface modification of QD nanoparticles with multidentate dithiol/zwitterion copolymer ligands[45] to develop a universal and tunable platform for the oriented immobilization of whole antibodies to QDs. The approach relies upon a controlled substitution of some of the ligand's thiol groups to enable the covalent binding of an intermediate protein A layer that subsequently supports oriented Ab immobilization. Relying upon some of the ligand's anchoring groups for bioconjugation represents a change in paradigm for which we demonstrate feasibility and robustness. The comparative advantages of this strategy over random antibody immobilization approaches are highlighted by deploying a set of versatile characterization assays to determine both the total number of surface-bound biomolecules and the fraction of "functional" Ab molecules per dot (an innovative "on-dot" ELISA type of assay is presented). The QD−antibody nanoconstructs are further characterized with regard to their size, optical properties, and surface potential. Efforts were dedicated to the evaluation of the long-term nonspecific interactions of the nanoconjugates with living cells and the eventual effects of this long-term exposure onto cell metabolism (toxicity). Such considerations are an evident prerequisite for in vivo applications of this technology, where nonspecific interactions with nontarget organs and cells are, together with biospecific recognition and lack of toxicity, a definitive must. Proof-of-concept cellular labeling applications of these nanobioconstructs are thereafter presented, including immunolabeling of extra- and intracellular targets and tracking of cell receptor internalization in live cells (cannabinoid receptor 1).[46]

2. RESULTS AND DISCUSSION

2.1. Characterization of the QD Nanobioconjugates.

In this work, 7−8 nm diameter core/shell CdSe/CdS/ZnS nanoparticles (emission maxima, λ_{max}, at around 580 or 610 nm) were synthesized following well-established protocols.[45,47] These nearly size monodisperse nanocrystals were thereafter transferred to aqueous media by ligand exchange with a multidentate dithiol/zwitterion copolymer previously developed in our group.[45] The ligand exchange process relies upon "dynamic" binding interactions between multiple dithiol groups present in the ligand and Zn^{2+} surface ions. These noncovalent interactions repeated along the ligand chain length by multiple attaching dithiol points confer high stability to the capped nanoparticles in a remarkable wide range of pHs (3−13) while concomitantly preserving most of the photoluminescence characteristics of the parent nanocrystals (typical QD quantum yield in water: 30−40%). The robust surface passivation obtained with the zwitterionic ligand[45] together with the fouling-resistant character of the so-capped zwitterionic nanoparticles and the availability of multiple dynamic anchoring points to the QD surface have provided a fertile ground for the development of a versatile bioconjugation platform. Indeed, it has been demonstrated that zwitterionic polymers have antifouling qualities,[48−50] a prerequisite for any in vivo application of QDs, as well as less detrimental effects than PEG on the functionality of surrounding proteins.[51] These properties are of pivotal relevance in our case since the zwitterionic chains (93 molar % of the ligand) will be in close proximity to any QD-bound biomolecule. Departing from these zwitterionic QDs, we exploited the dynamic interactions of the ligand's dithiol units with the QD surface to covalently immobilize a layer of protein A via sulfhydryl−maleimide

DOI: 10.1021/acsami.5b09777
ACS Appl. Mater. Interfaces XXXX, XXX, XXX−XXX

chemistry (Figure 1). For that, surface-accessible lysine residues in the protein were modified with the heterobifunctional

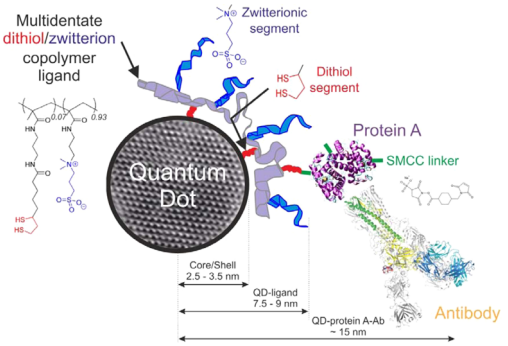

Figure 1. Schematics of the proposed QD bioconjugation strategy to produce QD nanoconstructs functionalized with well-oriented, fully functional antibodies. Core/shell QD nanocrystals are brought to aqueous media by ligand exchange with a multidentate dithiol/zwitterion copolymer ligand. The neutrally charged zwitterionic segments of the ligand confer solubility and an antifouling character to the nanoparticles. The dithiol segments are the ligand's anchoring points to the QD surface and are also effectively exploited for bioconjugation. A protein A layer is built on the QD surface by covalent binding between some of the ligand's sulfhydryl groups and maleimide moieties introduced in protein A after reaction with the SMCC linker. Antibody immobilization to the QD−protein A nanoconstructs occurs via simple incubation with whole, tag-free, unmodified antibodies. Protein A specifically binds antibodies through their Fc fragment, thus enabling antibody retention on the QD surface while preserving its 3D conformation, flexibility, and antigen recognition site. QD−protein A nanoconjugates constitute a universal platform for the surface immobilization of antibodies to QDs that expands the palette of nano(bio)conjugation options relevant to unresolved biological questions.

(amine-to-sulfhydryl) linker SMCC thereby introducing maleimido groups to the protein. At a 1:5 protein/SMCC molar ratio and supposing a Poissonian distribution for the protein−SMCC reaction, we could theoretically maximize the conjugation efficiency (i.e., almost all protein molecules conjugated with the linker) without significantly altering the 6 Ab binding regions that recombinant protein A has, as it will be later demonstrated. Various molar excess ratios of protein to QD were considered. Conversely to what has been vastly reported concerning biomolecule conjugation to QDs, our concept has several advantages: (1) no need for ligand activation (e.g., EDC/NHS); (2) no unwanted cross-linking between QDs or proteins (e.g., bis-NHS linkers); (3) no side-reactions, as the ones occurring with NHS ester linkers[45] that led to the spurious formation of thioesters; (4) all modification takes place on the protein intermediate layer; modification is orthogonal (excludes linker-induced protein cross-linking); (5) covalent binding of the protein to the QD ligand as opposed to electrostatic interactions with the QD surface (leucine zipper[10,20,35,52] or His tag[25]) for which competitive displacement by serum proteins could occur; and (6) protein A has some advantages over protein G, like its 6 Ab-binding sites as compared to 2 for protein G and its higher preference for the Fc fragment of Abs, thus promoting oriented Ab immobilization (protein G binds both, Fc and Fab Ab fragments[53]). Moreover, when a broader Ab binding specificity was required, protein A was replaced by recombinant protein A/G, the whole with similar results. Last but not least, this concept is directly transferrable to the immobilization of other proteins, to streptavidin-based systems or to other thiol-exhibiting platforms.

2.1.1. Immobilized Protein A Amount. The number of protein molecules immobilized per dot was determined by using a protein quantification assay, the BCA (bicinchoninic acid) test, applied to the recovered, unbound protein after conjugation (Figure S1). As indicated in Figure 2, panel A, the number of protein molecules immobilized per dot increases at increasing molar ratios of protein to QD, with approximately 10 protein A molecules per dot at a 30 molar excess. Estimates on the number of protein molecules required to saturate the QD surface range from 10 to 28−40 for QDs without and with ligands, respectively (Annex SI). Indeed, even at a 1:30 QD:protein A ratio and with 10 protein molecules per dot, surface saturation has not been reached (Figure 2A). Noticeably, though, the mean hydrodynamic diameter of the 1:30 QD−protein A nanoconstructs was found to be of 38 ± 8 nm versus the 16 ± 0.8 nm of the QD−zwitterionic ligand nanoparticles (Table 1). The prominent increase in the overall diameter of the nanoconstructs is then much larger than what could be expected from a protein of 5 nm diameter. This may

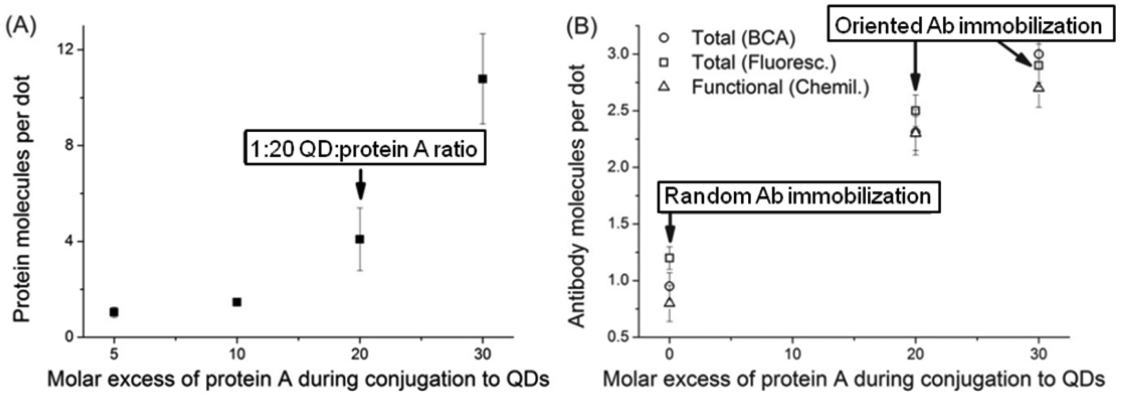

Figure 2. (A) Protein A and (B) Ab molecules immobilized per dot as a function of the molar excess of protein A employed during bioconjugation to QDs. (B) Random and oriented Ab immobilization strategies are compared at a 1:4 QD:Ab ratio. Random Ab immobilization refers to the direct covalent binding of the Ab to the QD ligand, that is, no protein A layer is added. The total immobilized antibody amount is quantified via the BCA test and by fluorescence, while the number of "functional" antibody per QD was obtained by chemiluminescence relying on a novel "on-dot" ELISA type of assay.

DOI: 10.1021/acsami.5b09777
ACS Appl. Mater. Interfaces XXXX, XXX, XXX−XXX

Table 1. Diameter of QD Nanoconstructs As Determined by DLS[a]

	diameter (mean ± STD) [nm]			
bioconjugate	fresh		six-month old	
QD−zwitterionic ligand	16 ± 0.8		17 ± 1.6	
QD−protein A	1:20 QD:protein A	1:30 QD:protein A	1:20 QD:protein A	1:30 QD:protein A
	22.4 ± 2	38 ± 8	19.4 ± 1	27 ± 5
QD−protein A−Ab	29 ± 2	54 ± 18	22 ± 4	61 ± 16

[a]Two QD:protein A ratios during bioconjugation were used: 1:20 and 1:30. The QD:Ab ratio was kept constant at 1:4. Freshly-prepared and six-month old samples were measured. The latter were stored at 4 °C for six months in a buffer containing neither additives nor preservatives.

be explained by the loss upon immobilization of the rather globular conformation that characterizes proteins in solution and by the consequent adoption of a more extended conformation as more protein needs to fit among the hydrated zwitterionic chains. On the other hand, QD−protein A nanoconstructs obtained at 1:20 ratio were characterized by 4−5 protein molecules per dot (Figure 2A) and yielded mean diameters of 22.4 ± 2 nm (Table 1). This size gain is more adapted to future applications where constraints apply to the overall size of the nanoparticles. A 1:20 QD:protein A ratio was therefore retained for the posterior affinity-driven immobilization of Abs to QDs; the 1:30 ratio was only kept with characterization purposes. Finally, regarding the size of the QD−protein A conjugates, DLS measurements showed predominantly monomodal, small size populations (Annex SII). By taking into account the high sensitivity of DLS to aggregates, this suggests a high colloidal stability of the QD−protein A nanoconstructs.

2.1.2. Immobilized Antibody Amount and Functionality/Specificity. Rabbit IgGs (for which protein A has a good affinity) were immobilized on the QD−protein A nanoconstructs (QD:Ab ratio of 1:4) by simple incubation followed by separation (ultracentrifugation). The QD−protein A−Ab nanoconstructs were characterized as per the number of immobilized Ab molecules per dot (BCA and fluorescence measurements of Ab-fluorophore bound to QD−protein A dots) as well as regarding the effective number of functional Ab molecules among those immobilized (chemiluminescence), both for random and oriented Ab immobilization strategies. Random antibody immobilization refers to the immobilization of the Ab without an intermediate protein A layer (QD:protein A ratio is 1:0). In that case, the Abs are first modified with the SMCC linker and thereafter bound to the ligand's thiols as for the protein A layer. As shown in Figure 2, panel B, BCA and fluorescence quantification of the total number of Ab molecules immobilized per QD consistently show Ab/QD ratios of about 1 for the random conjugation, and ∼2.4 and 3 for the oriented immobilization cases (1:20 and 1:30 QD:protein A ratios, respectively). Considering that the QD:Ab molar ratio is of 1:4 in all cases, the yield of the Ab immobilization reaction is of 25, 60, and 75%, respectively, for the above-mentioned cases. The oriented immobilization strategy is then more effective than the random approach at retaining higher fractions of the available Ab on the QD surface. Besides amount, the critical issue is the functionality of those immobilized Abs. To that respect, qualitative assays with agarose beads provided the first insights into conserved Ab function and specificity after immobilization to QDs (Figure S2). Noteworthy, these 1−3 Ab molecules per dot appear to fall in a range for which hydrophobic Ab−Ab or Ab−(QD−protein A) interactions are not prevalent. If they were so, gradual Ab denaturation and consequent loss of Ab function would be observed.[54−56] As it will be further discussed in reference to the functionality of the nanobioconjugates, this is not the case.

To quantify the fraction of "functional" antibody among those immobilized, a novel "on-dot" ELISA type of assay based on chemiluminescence was developed (see Experimental Section for a detailed description). The estimation of functional Ab bound to the QD surface this test provided highlighted the advantages of oriented over random immobilization approaches: while 2−3 functional Ab molecules could be obtained by adopting a protein A intermediate layer in the OI case, less than one functional Ab per dot resulted after random immobilization (Figure 2B). The overall "functionality" yield of the QD−Ab reaction is then of ∼50−75% for the OI approach versus ∼25% for the random platform. Similar findings regarding amount and function of antibodies bound to surfaces in random and oriented ways were reported by Wang et al.[57] The number of Ab molecules per dot is typically provided in the literature either as a measured value or as an estimation. Contrarily, the functionality of the QD-bound Ab (or target-specific species) is often missing. For instance, Lee et al.[58] reported ∼6−7 Ab molecules per dot relying upon a random immobilization strategy. Working with avidin as binding protein for the Abs, Goldman et al.[20] reported 0.5 antibodies per QD (DHLA ligand, avidin surface-immobilized to the QDs via electrostatic self-assembly). Variations of this work followed for which 3−5 Ab molecules per dot could be obtained by using protein G-leucine zipper as intermediate protein.[10,33] In these works, though, the fraction of functional Ab is not provided. Departing from published QD bioconjugation protocols and by applying an SDS-PAGE electrophoresis approach, Pathak et al.[41] succeeded (and were possibly the first) at estimating the number of functional Ab bound to QDs in a random conformation or via a streptavidin intermediate layer. The authors found that random Ab conjugation to nanoparticles performed with a commercial kit (Invitrogen) that requires the prereduction of Ab disulfide bonds resulted in less than 0.1 functional Ab per dot.[41] The situation was better for the streptavidin case, with 1.3 functional Ab per dot, but still the Ab content and functionality were found to be significantly lower than previously estimated. With 2−3 "functional" Abs per dot and a simple bioconjugation approach, our platform has the versatility and attributes often sought for to effectively approach biological and diagnostics issues with QD nanobioconjugates.

Finally, referring to the random Ab immobilization case, in our hands, this strategy resulted in about one Ab molecule per dot (Figure 2B; BCA and fluorescence data) and in a ∼75% functionality retention after conjugation to QDs (Figure 2B; chemiluminescence data). This is *per se* an undoubtedly positive feature since it demonstrates the relative facility of Ab conjugation to QDs capped with a dithiol/zwitterion

DOI: 10.1021/acsami.5b09777
ACS Appl. Mater. Interfaces XXXX, XXX, XXX−XXX

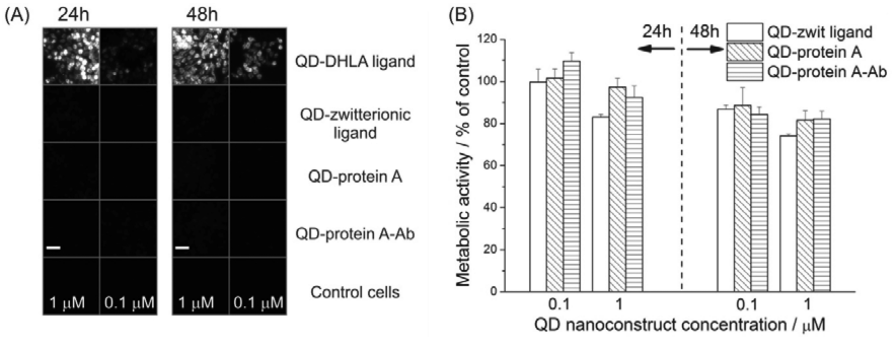

Figure 3. Numbers of (A) protein A and (B) Ab molecules (A) aonspecific interactions of QD nanoconstructs with HeLa cells in culture after 24 and 48 h incubation. Epifluorescence microscopy images of fixed cells after incubation with the nanoconjugates at 0.1 and 1 μM concentration (QD λ_{max} = 610 nm). All constitutive layers of the QD bioconjugates were evaluated. In addition, QDs with an alternative ligand, DHLA (dihydrolipoic acid), were assayed with comparative purposes. Control cells are cells not exposed to the QD nanoconstructs but otherwise equally treated. Scale bar: 50 μm. (B) Metabolic activity of HeLa cells after 24 and 48 h of exposure to 0.1 and 1 μM QD nanoconstructs under cell culture conditions. The metabolic activity is expressed as a percentage of the control (unperturbed cells).

copolymer ligand as well as the strengths of the bioconjugation protocol with regard to Ab functionality retention.

2.1.3. Size, Stability, and Photoluminescence Properties. As detailed in Table 1, there is a consistent nanoparticle size increase following the immobilization of the protein and Ab layers. The QD−zwitterionic ligand diameter (as measured by DLS over a range of scattering angles) increases up to ∼23 nm by the addition of a protein A layer (QD:protein A = 1:20) and reaches a final ∼30 nm after immobilization of the Ab layer. For a comparison, our random Ab immobilization approach produced nanoconjugates of 24 ± 3.6 nm diameter. On the other hand, utilizing QD:protein A ratios of 1:30, the overall nanoparticle sizes after incorporation of each layer are bigger (∼50−60 nm final after Ab binding) and less monodisperse (bigger error bars; Annex SII) than for the 1:20 case. These size gains are nevertheless typically smaller than what could be obtained with PEG-based amphiphilic polymer ligands.[59] After six months of storage at 4 °C, particle size remained approximately within the initial values ± STD in both, 1:20 and 1:30 QD:protein A cases (Table 1). Taken together, these findings reveal the largely monodispersed and small-size characteristics (∼30 nm diameter) of the QD nano(bio)-construct populations obtained at 1:20 QD:protein A ratios. The stability retention of these nanobioconstructs was not only limited to colloidal stability, but also the biofunctional QD−protein A−Ab particles preserved their fluorescence quantum yield (variations limited to ±20%) and their target specificity after half year storage at 4 °C in a buffer solution free of preservatives or any other additive. Similarly, 6-month-old QD−protein A nanoconstructs could be satisfactorily bound to Abs and used to specifically recognize their targets in biological experiments (Figure S3).

Finally, for the CdSe/CdS/ZnS dots here employed, both the absorbance (Figure S4A) and photoluminescence (PL; Figure S4B) spectra of the bioconjugated QDs remained unchanged as compared to the unconjugated QDs. This is valid for the two types of QDs (λ_{max} ≈ 580 or 610 nm) employed along this work. In particular for the PL spectra, neither bands' shifts nor asymmetry features could be evidenced in contrast to recent reports for CdSe(Te)/ZnS dots randomly coupled to Abs.[60]

2.2. Cell−Nanoparticle Interactions. *2.2.1. Nonspecific Cell−Nanoconjugate Interactions.* The following step in the characterization of the QD nanoconstructs dealt with the evaluation of the nonspecific interactions between cells in culture and the bioconjugates present in solution at different concentrations. In parallel, changes in cell metabolism induced by long-term incubation periods with the nanoconjugates were carefully screened. As observed in Figure 3, panel A, the cell−nanomaterial interactions were such that the nonspecific adsorption of QD−protein A−Ab bioconjugates onto HeLa cells went rather unnoticeable even after 48 h incubation with QD concentrations as high as 1 μM. The mean fluorescence per field of view of the QD-exposed samples remained at the level of the blank control with cells only (p = 0.05; see Experimental Section and Annex SIII for details). This stood true also for the bioconjugate underlayers, that is, the QD−zwitterionic ligand and QD−protein A layers, which could be partly exposed in the final QD−protein A−Ab bioconjugates and hence play a role in the nonspecific interactions. After 48 h of incubation with HeLa cells, the mean fluorescence intensities of the samples exposed to the various QD constitutive layers are similar (p = 0.01; Annex SIII). This has a correspondence with the similar zeta potentials obtained for these samples: all QD nanoconstructs' constitutive layers have zeta potentials of about −9 ± 1.3 mV in 50 mM HEPES, 100 mM NaCl, pH 7.5 buffer. Since (i) protein/Ab denaturation upon surface binding would favor unspecific hydrophobic interactions with cell membrane lipids and (ii) partial QD ligand instabilities resulting from incubation in a complex medium (such as the cell culture one) and at 37 °C would prompt a loss of colloidal stability, the minimal retention of QD bioconjugates on HeLa cell surfaces after incubation is an encouraging feature denoting the robust and stable character of these nanobioconstructs. While the negatively charged QD−DHLA ligand nanoparticles are increasingly retained on the cell surface as incubation time advances, their QD−zwitterionic ligand counterparts show almost no change in nonspecific adsorption over the time periods here considered. This suggests some level of long-term stability of the QD−zwitterionic ligand nanoparticles under cell culture conditions. With similar arguments, the same stands for the QD bioconjugates and represents, together with the cell metabolism data discussed below, a required preamble for long-term in vivo applications of biofunctional QD nanoparticles.

2.2.2. Cell−Nanoconjugate Interactions and Their Effect onto Cell Metabolism. The exposure of HeLa cells to QD nanobioconstructs under cell culture conditions resulted in a partial reduction of cellular metabolic activity, as determined by

DOI: 10.1021/acsami.5b09777
ACS Appl. Mater. Interfaces XXXX, XXX, XXX−XXX

the MTT (thiazolyl blue tetrazolium bromide) test (Figure 3B), though still with elevated ~80% metabolic activity retention levels after 48 h incubation at 1 μM. The capacity of the QD-exposed cells to reduce the tetrazolium salt MTT in active mitochondria via various dehydrogenase enzymes[61] diminishes with time and with QD concentration. At 1 μM, unconjugated QDs are more prone to affect cell metabolism than QDs conjugated with protein A or protein A−Ab ($p < 0.05$). Within a similar range of QD concentrations (0.1−2 μM) and incubation time (48 h), Yu et al.[59] reported cell death values between 10 and 15% for QDs modified with a PEG-based amphiphilic polymer coating that approach our observations. The MTT relative viability values obtained by Wang et al.[62] are also similar to ours. To our best knowledge, these levels of cellular metabolic activity retention (~80%) after exposure to CdSe/CdS/ZnS nanoparticles are high compared to available literature.[63,64] Noteworthy, our findings point at a diminution of cytotoxicity when nanoparticles are surface-modified with biomolecules compared to unconjugated QDs. This may in part be due to the higher size of the QD bioconjugates as compared to the parent QD zwitterion nanoparticles. In any case, standard biological imaging studies typically require much shorter exposure times (10−15 min) and lower concentrations (0.1−0.3 μM). The effects of the nanobioconstructs on cell metabolism should thus be minimal in these applications.

2.3. Biological Applications of QD Nanoconstructs. *2.3.1. Labeling of Extra- and Intracellular Markers in Fixed Cells.* The ability of the QD nanoconstructs to detect cell membrane proteins in fixed, but no permeabilized cells were selected as a first stage validation of the nanoconjugates in model biological systems. MCF-7 cells expressing E-cadherin were derived from a breast carcinoma. Cadherins are transmembrane proteins that mediate cell−cell adhesion processes. Changes in the function and expression levels of cellular adhesion molecules have been correlated with the progression and invasiveness of a variety of tumors.[65−70] Preliminary experiments had validated the specificity of a commercial goat polyclonal anti E-cadherin antibody (R&D Systems). Because of its superior affinity for goat antibodies, protein A/G was here employed to generate QD−protein A/G−anti E-cadherin nanoconstructs. As shown in Figure 4, panels A−C, immunofluorescence detection of E-cadherin with QD−protein A/G−anti E-cadherin nanoconstructs resulted in clear, specific membrane labeling in confocal scans. On the other hand, when cells were exposed to QD−protein A/G bioconjugates (blank control), the interactions of the QD protein layer with the fixed cells' surface were negligible (Figure 4C).

A more challenging case in QD-based immunolabeling applications is the proper visualization of intracellular structures in fixed and permeabilized cells. QD−protein A−anti β-tubulin nanoconstructs were effective at labeling the cytoskeleton β-tubulin protein in formaldehyde-fixed and permeabilized HeLa cells (Figure 4D). The nanoconjugates enabled a good visualization of the cytoskeleton microtubules (Figure 4D) and had minimal unspecific adsorption in all negative controls tested: Primary Ab + QD−protein A−secondary antibody not specific for the primary; QD−protein A alone; and NO primary Ab + QD−protein A−secondary antibody specific for the primary (the last one shown in Figure 4E). In both, intra- and extracellular immunohistochemistry applications, the blank (QD−protein A layer) and negative (QD−protein A−antibody that does not recognize the target) controls showed

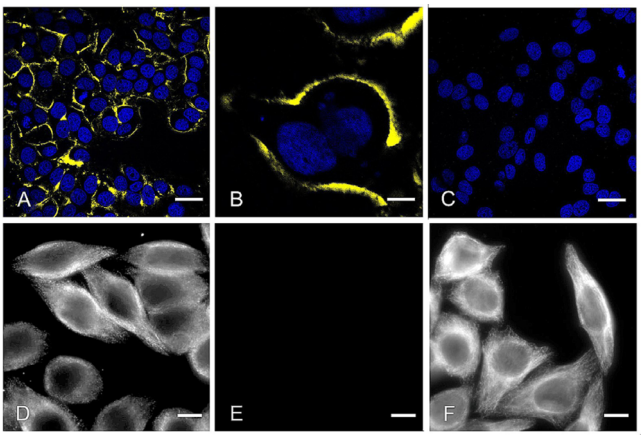

Figure 4. Extracellular E-cadherin labeling with QD nanoconjugates on MCF-7 cells. Confocal microscopy images of fixed cells. (A, B) MCF-7 cells exposed to 1 μM QD−protein A/G−anti E-cadherin nanoconstructs. (C) Control sample exposed to 1 μM QD−protein A/G nanoconstructs. Cell nuclei stained with DAPI. QD signal is confined to the cell−cell junctions in E-cadherin positive MCF-7 cells (A, B), whereas the control with QD−protein A/G nanoconjugates is not labeled (C). Scale bar: 20 μm in panels A and C; 5 μm in panel B. QD λ_{max} = 580 nm. Intracellular β-tubulin (cytoskeleton) labeling on HeLa cells. Epifluorescence microscopy images of fixed and membrane-permeabilized cells. (D) HeLa cells exposed to 0.2 μM QD−protein A−anti β-tubulin. (E) Negative control with 0.2 μM QD−protein A−anti mouse (rabbit) nanoconstructs. Here, in the absence of the primary antibody (mouse anti β-tubulin), there is no QD retention on the surface. (F) Positive control with primary antibody coupled to antimouse Alexa 555. Scale bar: 10 μm. QD λ_{max} = 610 nm.

fluorescence intensities close to autofluorescence levels. In particular, when a primary Ab is used in immunofluorescence, the negative control (QD−protein A−secondary antibody not specific for the primary) reflects not only the absence of a cross-talk between seemingly nonreactive antibodies, but also the absence of an interaction between the underlying protein A layer and the cell-bound primary Ab. This is of critical importance in cases where QDs are to be conjugated to secondary Ab and used in conjunction with other nanoconjugates and primary Abs in multiplexing applications.

2.3.2. Tracking Internalization Dynamics of Membrane Receptors in Live Cells. The final aim in the development of QD nanobioconjugates is the obtainment of highly specific, stable, and nontoxic probes capable of sensitive in vivo detection of target molecules. In this work, an approximation to the in vivo case is presented that focuses on the identification and follow-up of cell receptor dynamics in live cells. HEK cells stably expressing the type-1 cannabinoid (CB1) receptor fused to GFP and FLAG tags on its intra- and extracellular domains, respectively, were utilized as model cells.[22,46] The cannabinoid receptor 1, the brain target of marijuana and endocannabinoid ligands, is one of the most abundant G protein-coupled receptors in the central nervous system, well recognized as an important modulator of synaptic plasticity and neuronal development.[66,68] The receptor has been shown to permanently and constitutively cycle between plasma membrane and endosomes in HEK cells, having a predominantly intracellular localization at steady state.[46] Membrane-localized CB1 receptors were first labeled by incubating cells with 0.02 μM QD−protein A−anti FLAG nanoconstructs for 10 min at 4 °C, an unpermissive temperature for receptor internalization. Once

DOI: 10.1021/acsami.5b09777
ACS Appl. Mater. Interfaces XXXX, XXX, XXX−XXX

unbound QDs were rinsed off and temperature was rapidly raised to 37 °C, receptor internalization started and could be tracked. To gain insight into time zero nanoconjugate−cell receptor interactions, cells were fixed and observed in an epifluorescence microscope before the onset of internalization. At the zero time point, the specific binding of QD−protein A−anti FLAG nanoconstructs to the FLAG tag-bearing CB1 receptor was evidenced by the colocalization of QD and GFP signals on the cell membrane (Figure 5A,B). When cells were

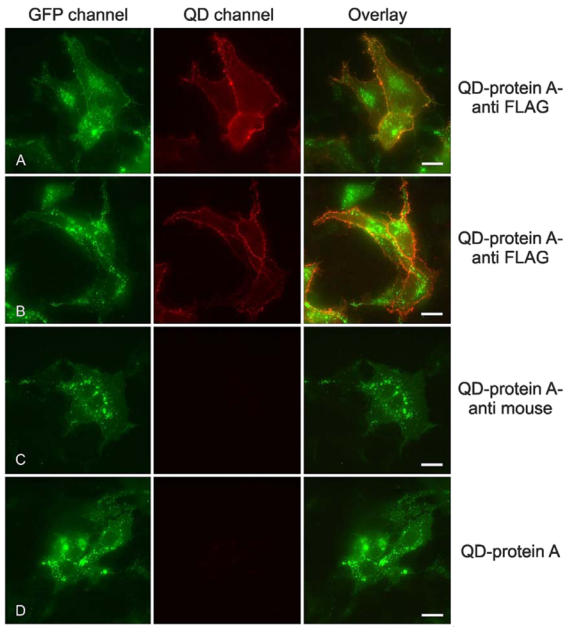

Figure 5. CB1 receptor labeling at the plasma membrane in live HEK cells. Cells stably express the CB1 (cannabinoid B1) receptor coded to a GFP (green fluorescent protein) intracellular terminus and an extracellular FLAG tag. Epifluorescence microscopy images taken after cell exposure to (A, B) QD−protein A−anti FLAG, (C) QD−protein A−anti mouse, or (D) QD−protein A bioconjugates. Live cells were exposed to 0.05 μM QD nanoconstructs during 10 min at 4 °C, rinsed, and then fixed for observation. GFP and QD channels are shown together with their overlay image where distinctive membrane labeling is observed for QD bioconjugates bearing the anti-FLAG antibody (A, B). Unspecific binding is negligible in the negative controls (C, D). Scale bar: 20 μm. QD λ_{max} = 610 nm.

incubated with the negative controls QD−protein A−anti mouse or QD−protein A nanoconstructs, no labeling was detected (Figure 5C,D, respectively). Upon a rapid temperature increase to 37 °C after QD labeling, the onset of receptor internalization was prompted: the initially membrane-confined QD signal (Figure 6A) slowly moves in, and after approximately 10 min, the first signs of intracellular presence of the QD nanoconstructs are noticed (Figure 6B). This QD-tracked receptor internalization proceeds over time, with substantial mobility of the QD bioconjugates inside the cytosol (S.Video1 and S.Video2). Thirty minutes after the end of the incubation period with the QD nanoconstructs, the totality of the QD signal was located in the cytosol, demonstrating a complete internalization of the QD-labeled receptors (Figure 6C). This model biological system demonstrates the quick (∼10 min) and specific target recognition capacity of the QD nanobioconjugates here developed as well as the active cellular uptake of receptor-bound QD nanoparticles in live cells. Furthermore, QDs preserved their fluorescence properties as

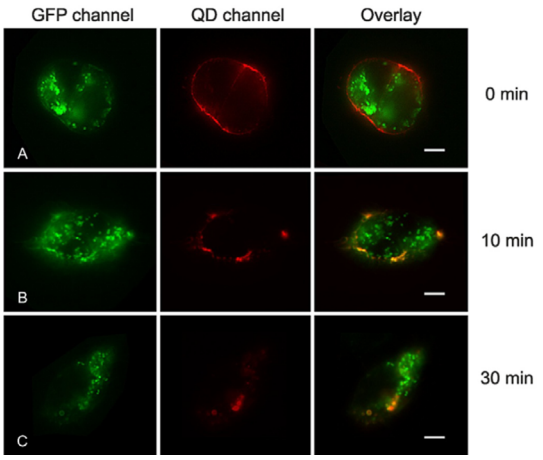

Figure 6. Tracking CB1 receptor internalization in live HEK cells. At the zero time point after QD labeling, the QD signal is restricted to the plasma membrane (A). After 10 min cell incubation at 37 °C, the first hints of receptor internalization are perceived (B) with QD signals being located in the cytoplasm near the cell membrane. After 30 min (C), the QD signal comes exclusively from the organelles in the cytosol, thus implying a complete internalization of the receptor-bound QD bioconjugates that were initially located at the cell membrane. Epifluorescence images acquired with the bicolor system. GFP and QD channels are presented together with their overlay image. Scale bar: 5 μm. QD λ_{max} = 610 nm.

far as 7 h after the onset of internalization (Figure S5). Fluorescence stability is a reflection of conserved colloidal stability over time in the endosomes, which are acidic organelles with an intralumen pH of 5−6. Last but not least, these QD nanoconstructs remained colocalized with GFP over time, thus proving the lack of dissociation from the CB1 receptor, which could be prompted by the denaturation of the QD-bound Ab in the cellular milieu or by active cellular processes.

3. CONCLUSIONS AND PERSPECTIVE

In this work, a versatile strategy for the surface functionalization of QD nanoparticles with whole, unmodified antibodies is presented together with a detailed characterization of the extent of such a biofunctionalization. This strategy brings about a paradigm change: the ligand's thiol anchoring groups can also be exploited for bioconjugation without jeopardizing the physicochemical properties of the resulting QD nanoconjugates. Well-known oriented immobilization principles are deployed that result in ∼2−3 fully functional Ab molecules per dot departing from a universal platform, QD−protein A nanoconstructs, and relying upon simple protocols. These nanobioconjugates were effective at labeling intra- and extracellular targets in fixed cells and demonstrated utility at the identification and posterior tracking of CB1 receptor proteins in live cells. Moreover, the nanoconjugates retained colloidal stability and target-biospecificity for up to six months and displayed very low nonspecific binding to cells as well as minimal toxicity after 48 h incubation. On the whole, these results provide a sound ground for future applications of the virtues of QDs to the resolution of biological problems, for example, in-depth analysis of membrane protein trafficking or detection of cell markers of low levels of expression.

DOI: 10.1021/acsami.5b09777
ACS Appl. Mater. Interfaces XXXX, XXX, XXX−XXX

4. EXPERIMENTAL SECTION

Core/shell CdSe/CdS/ZnS nanoparticles were synthesized and transferred to aqueous solution by ligand exchange with the multidentate dithiol/zwitterion ligand as described in Giovanelli et al.[45] The covalent binding of a protein A intermediate layer to the QDs was performed by simple incubation of SMCC-derivatized protein A (1:5 protein:linker molar ratio) with the ligand-capped nanoparticles in 50 mM HEPES, 100 mM NaCl, pH 6.5 buffer for 1 h. Besides the characterization experiments for which variable QD:protein A ratios were employed, a 1:20 molar ratio was the norm along this work. Unreacted protein A was separated via two rounds of ultracentrifugation at 151 000*g* for 25 min. Affinity-binding of Abs to the QD−protein A nanoconstructs occurred by simple incubation at a 1:4 QD:Ab molar ratio in 50 mM HEPES, 100 mM NaCl, pH 8.5 buffer for 1.5 h. Unbound Ab was separated as done for protein A. For a detailed description of the methodology, see the Supporting Information.

■ ASSOCIATED CONTENT

Supporting Information

The Supporting Information is available free of charge on the ACS Publications website at DOI: 10.1021/acsami.5b09777.

Detailed experimental procedures; additional data of optical properties, in vitro functionality assay, evaluation of functionality after six months storage, long-term receptor tracking, supporting videos (PDF)

Time-lapse imaging of internalized FLAG-CB1-GFP receptor traffic in HEK cells after labeling with QD−protein A−anti FLAG conjugates (AVI)

Time-lapse imaging of internalized FLAG-CB1-GFP receptor traffic in HEK cells after labeling with QD−protein A−anti FLAG conjugates (AVI)

■ AUTHOR INFORMATION

Corresponding Author

*E-mail: thomas.pons@espci.fr.

Notes

The authors declare no competing financial interest.

■ ACKNOWLEDGMENTS

This work was supported by the NanoCTC (ANR-10-Nano-05) grant of the "Investissement d'Avenir" program managed by the French Agence Nationale de la Recherche. The SIMM-PPMD and LBC laboratories at ESPCI are acknowledged for the sharing of their equipment.

■ REFERENCES

(1) Kairdolf, B. A.; Smith, A. M.; Stokes, T. H.; Wang, M. D.; Young, A. N.; Nie, S. Semiconductor Quantum Dots for Bioimaging and Biodiagnostic Applications. *Annu. Rev. Anal. Chem.* **2013**, *6*, 143−62.

(2) Petryayeva, E.; Algar, W. R.; Medintz, I. L. Quantum Dots in Bioanalysis: A Review of Applications across Various Platforms for Fluorescence Spectroscopy and Imaging. *Appl. Spectrosc.* **2013**, *67* (3), 215−252.

(3) Domaille, D. W.; Que, E. L.; Chang, C. J. Synthetic Fluorescent Sensors for Studying the Cell Biology of Metals. *Nat. Chem. Biol.* **2008**, *4* (3), 168−175.

(4) Lippincott-Schwartz, J.; Patterson, G. H. Development and Use of Fluorescent Protein Markers in Living Cells. *Science* **2003**, *300* (5616), 87−91.

(5) Resch-Genger, U.; Grabolle, M.; Cavaliere-Jaricot, S.; Nitschke, R.; Nann, T. Quantum Dots Versus Organic Dyes as Fluorescent Labels. *Nat. Methods* **2008**, *5* (9), 763−775.

(6) Mattoussi, H.; Palui, G.; Na, H. B. Luminescent Quantum Dots as Platforms for Probing in Vitro and in Vivo Biological Processes. *Adv. Drug Delivery Rev.* **2012**, *64* (2), 138−166.

(7) Medintz, I. L.; Uyeda, H. T.; Goldman, E. R.; Mattoussi, H. Quantum Dot Bioconjugates for Imaging, Labelling and Sensing. *Nat. Mater.* **2005**, *4* (6), 435−446.

(8) Michalet, X.; Pinaud, F. F.; Bentolila, L. A.; Tsay, J. M.; Doose, S.; Li, J. J.; Sundaresan, G.; Wu, A. M.; Gambhir, S. S.; Weiss, S. Quantum Dots for Live Cells, in Vivo Imaging, and Diagnostics. *Science* **2005**, *307* (5709), 538−544.

(9) Courty, S.; Luccardini, C.; Bellaiche, Y.; Cappello, G.; Dahan, M. Tracking Individual Kinesin Motors in Living Cells Using Single Quantum-Dot Imaging. *Nano Lett.* **2006**, *6* (7), 1491−1495.

(10) Jaiswal, J. K.; Mattoussi, H.; Mauro, J. M.; Simon, S. M. Long-Term Multiple Color Imaging of Live Cells Using Quantum Dot Bioconjugates. *Nat. Biotechnol.* **2002**, *21* (1), 47−51.

(11) Lidke, D. S.; Nagy, P.; Heintzmann, R.; Arndt-Jovin, D. J.; Post, J. N.; Grecco, H. E.; Jares-Erijman, E. A.; Jovin, T. M. Quantum Dot Ligands Provide New Insights into Erbb/Her Receptor-Mediated Signal Transduction. *Nat. Biotechnol.* **2004**, *22* (2), 198−203.

(12) Hildebrandt, N. Biofunctional Quantum Dots: Controlled Conjugation for Multiplexed Biosensors. *ACS Nano* **2011**, *5* (7), 5286−5290.

(13) Ji, X.; Peng, F.; Zhong, Y.; Su, Y.; He, Y. Fluorescent Quantum Dots: Synthesis, Biomedical Optical Imaging, and Biosafety Assessment. *Colloids Surf., B* **2014**, *124*, 132−9.

(14) Wegner, K. D.; Hildebrandt, N. Quantum Dots: Bright and Versatile in Vitro and in Vivo Fluorescence Imaging Biosensors. *Chem. Soc. Rev.* **2015**, *44*, 4792.

(15) Agrawal, A.; Zhang, C.; Byassee, T.; Tripp, R. A.; Nie, S. Counting Single Native Biomolecules and Intact Viruses with Color-Coded Nanoparticles. *Anal. Chem.* **2006**, *78* (4), 1061−1070.

(16) Blum, A. S.; Soto, C. M.; Wilson, C. D.; Whitley, J. L.; Moore, M. H.; Sapsford, K. E.; Lin, T. W.; Chatterji, A.; Johnson, J. E.; Ratna, B. R. Templated Self-Assembly of Quantum Dots from Aqueous Solution Using Protein Scaffolds. *Nanotechnology* **2006**, *17* (20), 5073−5079.

(17) Wu, S.-M.; Chen, J.; Ai, X.-X.; Yan, Z.-Y. Detection of Escherichia Coli in Drugs with Antibody Conjugated Quantum Dots as Immunofluorescence Probes. *J. Pharm. Biomed. Anal.* **2013**, *78*−*79* (0), 9−13.

(18) Wu, X.; Liu, H.; Liu, J.; Haley, K. N.; Treadway, J. A.; Larson, J. P.; Ge, N.; Peale, F.; Bruchez, M. P. Immunofluorescent Labeling of Cancer Marker Her2 and Other Cellular Targets with Semiconductor Quantum Dots. *Nat. Biotechnol.* **2002**, *21* (1), 41−46.

(19) Chen, C.; Peng, J.; Xia, H.-S.; Yang, G.-F.; Wu, Q.-S.; Chen, L.-D.; Zeng, L.-B.; Zhang, Z.-L.; Pang, D.-W.; Li, Y. Quantum Dots-Based Immunofluorescence Technology for the Quantitative Determination of Her2 Expression in Breast Cancer. *Biomaterials* **2009**, *30* (15), 2912−2918.

(20) Goldman, E. R.; Balighian, E. D.; Mattoussi, H.; Kuno, M. K.; Mauro, J. M.; Tran, P. T.; Anderson, G. P. Avidin: A Natural Bridge for Quantum Dot-Antibody Conjugates. *J. Am. Chem. Soc.* **2002**, *124* (22), 6378−6382.

(21) Howarth, M.; Takao, K.; Hayashi, Y.; Ting, A. Y. Targeting Quantum Dots to Surface Proteins in Living Cells with Biotin Ligase. *Proc. Natl. Acad. Sci. U. S. A.* **2005**, *102* (21), 7583−7588.

(22) Muro, E.; Pons, T.; Lequeux, N.; Fragola, A.; Sanson, N.; Lenkei, Z.; Dubertret, B. Small and Stable Sulfobetaine Zwitterionic Quantum Dots for Functional Live-Cell Imaging. *J. Am. Chem. Soc.* **2010**, *132* (13), 4556−7.

(23) Anikeeva, N.; Lebedeva, T.; Clapp, A. R.; Goldman, E. R.; Dustin, M. L.; Mattoussi, H.; Sykulev, Y. Quantum Dot/Peptide-Mhc Biosensors Reveal Strong Cd8-Dependent Cooperation between Self and Viral Antigens That Augment the T Cell Response. *Proc. Natl. Acad. Sci. U. S. A.* **2006**, *103* (45), 16846−51.

(24) Boeneman, K.; Delehanty, J. B.; Susumu, K.; Stewart, M. H.; Medintz, I. L. Intracellular Bioconjugation of Targeted Proteins with

DOI: 10.1021/acsami.5b09777
ACS Appl. Mater. Interfaces XXXX, XXX, XXX−XXX

Semiconductor Quantum Dots. *J. Am. Chem. Soc.* **2010**, *132* (17), 5975−5977.
(25) Medintz, I. L.; Clapp, A. R.; Mattoussi, H.; Goldman, E. R.; Fisher, B.; Mauro, J. M. Self-Assembled Nanoscale Biosensors Based on Quantum Dot Fret Donors. *Nat. Mater.* **2003**, *2* (9), 630−638.
(26) Susumu, K.; Medintz, I. L.; Delehanty, J. B.; Boeneman, K.; Mattoussi, H. Modification of Poly(Ethylene Glycol)-Capped Quantum Dots with Nickel Nitrilotriacetic Acid and Self-Assembly with Histidine-Tagged Proteins. *J. Phys. Chem. C* **2010**, *114* (32), 13526−13531.
(27) Dubertret, B.; Skourides, P.; Norris, D. J.; Noireaux, V.; Brivanlou, A. H.; Libchaber, A. In Vivo Imaging of Quantum Dots Encapsulated in Phospholipid Micelles. *Science* **2002**, *298* (5599), 1759−1762.
(28) Iyer, G.; Pinaud, F.; Xu, J.; Ebenstein, Y.; Li, J.; Chang, J.; Dahan, M.; Weiss, S. Aromatic Aldehyde and Hydrazine Activated Peptide Coated Quantum Dots for Easy Bioconjugation and Live Cell Imaging. *Bioconjugate Chem.* **2011**, *22* (6), 1006−1011.
(29) Liu, X.-L.; Peng, C.-W.; Chen, C.; Yang, X.-Q.; Hu, M.-B.; Xia, H.-S.; Liu, S.-P.; Pang, D.-W.; Li, Y. Quantum Dots-Based Double-Color Imaging of Her2 Positive Breast Cancer Invasion. *Biochem. Biophys. Res. Commun.* **2011**, *409* (3), 577−582.
(30) Bilan, R.; Fleury, F.; Nabiev, I.; Sukhanova, A. Quantum Dot Surface Chemistry and Functionalization for Cell Targeting and Imaging. *Bioconjugate Chem.* **2015**, *26*, 609.
(31) Montenegro, J. M.; Grazu, V.; Sukhanova, A.; Agarwal, S.; de la Fuente, J. M.; Nabiev, I.; Greiner, A.; Parak, W. J. Controlled Antibody/(Bio-) Conjugation of Inorganic Nanoparticles for Targeted Delivery. *Adv. Drug Delivery Rev.* **2013**, *65* (5), 677−88.
(32) Yezhelyev, M. V.; Qi, L.; O'Regan, R. M.; Nie, S.; Gao, X. Proton-Sponge Coated Quantum Dots for Sirna Delivery and Intracellular Imaging. *J. Am. Chem. Soc.* **2008**, *130* (28), 9006−9012.
(33) Goldman, E. R.; Anderson, G. P.; Tran, P. T.; Mattoussi, H.; Charles, P. T.; Mauro, J. M. Conjugation of Luminescent Quantum Dots with Antibodies Using an Engineered Adaptor Protein to Provide New Reagents for Fluoroimmunoassays. *Anal. Chem.* **2002**, *74* (4), 841−7.
(34) Jin, T.; Tiwari, D. K.; Tanaka, S.-i.; Inouye, Y.; Yoshizawa, K.; Watanabe, T. M. Antibody-Proteina Conjugated Quantum Dots for Multiplexed Imaging of Surface Receptors in Living Cells. *Mol. BioSyst.* **2010**, *6* (11), 2325−2331.
(35) Mattoussi, H.; Mauro, J. M.; Goldman, E. R.; Anderson, G. P.; Sundar, V. C.; Mikulec, F. V.; Bawendi, M. G. Self-Assembly of Cdse−Zns Quantum Dot Bioconjugates Using an Engineered Recombinant Protein. *J. Am. Chem. Soc.* **2000**, *122* (49), 12142−12150.
(36) Seo, J.-s.; Lee, S.; Poulter, C. D. Regioselective Covalent Immobilization of Recombinant Antibody-Binding Proteins a, G, and L for Construction of Antibody Arrays. *J. Am. Chem. Soc.* **2013**, *135* (24), 8973−8980.
(37) Chan, W. C. W.; Nie, S. Quantum Dot Bioconjugates for Ultrasensitive Nonisotopic Detection. *Science* **1998**, *281* (5385), 2016−2018.
(38) Han, H.-S.; Niemeyer, E.; Huang, Y.; Kamoun, W. S.; Martin, J. D.; Bhaumik, J.; Chen, Y.; Roberge, S.; Cui, J.; Martin, M. R.; Fukumura, D.; Jain, R. K.; Bawendi, M. G.; Duda, D. G. Quantum Dot/Antibody Conjugates for in Vivo Cytometric Imaging in Mice. *Proc. Natl. Acad. Sci. U. S. A.* **2015**, *112* (5), 1350−1355.
(39) Jennings, T. L.; Becker-Catania, S. G.; Triulzi, R. C.; Tao, G.; Scott, B.; Sapsford, K. E.; Spindel, S.; Oh, E.; Jain, V.; Delehanty, J. B.; Prasuhn, D. E.; Boeneman, K.; Algar, W. R.; Medintz, I. L. Reactive Semiconductor Nanocrystals for Chemoselective Biolabeling and Multiplexed Analysis. *ACS Nano* **2011**, *5* (7), 5579−5593.
(40) Li, C.; Ji, Y.; Wang, C.; Liang, S.; Pan, F.; Zhang, C.; Chen, F.; Fu, H.; Wang, K.; Cui, D. Brcaa1 Antibody- and Her2 Antibody-Conjugated Amphiphilic Polymer Engineered Cdse/Zns Quantum Dots for Targeted Imaging of Gastric Cancer. *Nanoscale Res. Lett.* **2014**, *9* (1), 244.
(41) Pathak, S.; Davidson, M. C.; Silva, G. A. Characterization of the Functional Binding Properties of Antibody Conjugated Quantum Dots. *Nano Lett.* **2007**, *7* (7), 1839−1845.
(42) Gersten, D. M.; Marchalonis, J. J. A Rapid, Novel Method for the Solid-Phase Derivatization of Igg Antibodies for Immune-Affinity Chromatography. *J. Immunol. Methods* **1978**, *24* (3), 305−309.
(43) Sonti, S. V.; Bose, A. Cell-Separation Using Protein-a-Coated Magnetic Nanoclusters. *J. Colloid Interface Sci.* **1995**, *170* (2), 575−585.
(44) Sukhanova, A.; Even-Desrumeaux, K.; Kisserli, A.; Tabary, T.; Reveil, B.; Millot, J.-M.; Chames, P.; Baty, D.; Artemyev, M.; Oleinikov, V.; Pluot, M.; Cohen, J. H. M.; Nabiev, I. Oriented Conjugates of Single-Domain Antibodies and Quantum Dots: Toward a New Generation of Ultrasmall Diagnostic Nanoprobes. *Nanomedicine (N. Y., NY, U. S.)* **2012**, *8* (4), 516−525.
(45) Giovanelli, E.; Muro, E.; Sitbon, G.; Hanafi, M.; Pons, T.; Dubertret, B.; Lequeux, N. Highly Enhanced Affinity of Multidentate Versus Bidentate Zwitterionic Ligands for Long-Term Quantum Dot Bioimaging. *Langmuir* **2012**, *28* (43), 15177−15184.
(46) Leterrier, C.; Bonnard, D.; Carrel, D.; Rossier, J.; Lenkei, Z. Constitutive Endocytic Cycle of the Cb1 Cannabinoid Receptor. *J. Biol. Chem.* **2004**, *279* (34), 36013−36021.
(47) Yu, W. W.; Peng, X. Formation of High-Quality Cds and Other Ii−Vi Semiconductor Nanocrystals in Noncoordinating Solvents: Tunable Reactivity of Monomers. *Angew. Chem., Int. Ed.* **2002**, *41* (13), 2368−2371.
(48) Cao, B.; Tang, Q.; Cheng, G. Recent Advances of Zwitterionic Carboxybetaine Materials and Their Derivatives. *J. Biomater. Sci., Polym. Ed.* **2014**, *25* (14−15), 1502−1513.
(49) Liu, P.; Skelly, J. D.; Song, J. Three-Dimensionally Presented Anti-Fouling Zwitterionic Motifs Sequester and Enable High-Efficiency Delivery of Therapeutic Proteins. *Acta Biomater.* **2014**, *10* (10), 4296−4303.
(50) Zhang, Z.; Chao, T.; Chen, S.; Jiang, S. Superlow Fouling Sulfobetaine and Carboxybetaine Polymers on Glass Slides. *Langmuir* **2006**, *22* (24), 10072−10077.
(51) Keefe, A. J.; Jiang, S. Poly(Zwitterionic)Protein Conjugates Offer Increased Stability without Sacrificing Binding Affinity or Bioactivity. *Nat. Chem.* **2011**, *4* (1), 59−63.
(52) Tran, P. T.; Anderson, G. P.; Mauro, J. M.; Mattoussi, H. Use of Luminescent Cdse−Zns Nanocrystal Bioconjugates in Quantum Dot-Based Nanosensors. *Phys. Status Solidi B* **2002**, *229* (1), 427−432.
(53) Derrick, J. P.; Wigley, D. B. The Third Igg-Binding Domain from Streptococcal Protein G: An Analysis by X-Ray Crystallography of the Structure Alone and in a Complex with Fab. *J. Mol. Biol.* **1994**, *243* (5), 906−918.
(54) Pavlickova, P.; Schneider, E. M.; Hug, H. Advances in Recombinant Antibody Microarrays. *Clin. Chim. Acta* **2004**, *343* (1−2), 17−35.
(55) Rayavarapu, R. G.; Petersen, W.; Ungureanu, C.; Post, J. N.; van Leeuwen, T. G.; Manohar, S. Synthesis and Bioconjugation of Gold Nanoparticles as Potential Molecular Probes for Light-Based Imaging Techniques. *Int. J. Biomed. Imaging* **2007**, *2007*, 1.
(56) Torcello-Gomez, A.; Santander-Ortega, M. J.; Peula-Garcia, J. M.; Maldonado-Valderrama, J.; Galvez-Ruiz, M. J.; Ortega-Vinuesa, J. L.; Martin-Rodriguez, A. Adsorption of Antibody onto Pluronic F68-Covered Nanoparticles: Link with Surface Properties. *Soft Matter* **2011**, *7* (18), 8450−8461.
(57) Wang, D.-S.; Chang, C.-C.; Shih, S.-C.; Lin, C.-W. An Ellipsometric Study on the Density and Functionality of Antibody Layers Immobilized by a Randomly Covalent Method and a Protein a-Oriented Method. *Biomed. Eng.* **2009**, *21* (05), 303−310.
(58) Lee, J.; Choi, Y.; Kim, K.; Hong, S.; Park, H.-Y.; Lee, T.; Cheon, G. J.; Song, R. Characterization and Cancer Cell Specific Binding Properties of Anti-Egfr Antibody Conjugated Quantum Dots. *Bioconjugate Chem.* **2010**, *21* (5), 940−946.
(59) Yu, W. W.; Chang, E.; Falkner, J. C.; Zhang, J.; Al-Somali, A. M.; Sayes, C. M.; Johns, J.; Drezek, R.; Colvin, V. L. Forming

DOI: 10.1021/acsami.5b09777
ACS Appl. Mater. Interfaces XXXX, XXX, XXX−XXX

Biocompatible and Nonaggregated Nanocrystals in Water Using Amphiphilic Polymers. *J. Am. Chem. Soc.* **2007**, *129* (10), 2871−2879.
(60) Torchynska, T. V.; Casas Espinola, J. L.; Díaz Cano, A.; Douda, J.; Gazarian, K. Emission of Cdse/Zns and Cdsete/Zns Quantum Dots Conjugated to Igg Antibodies. *Phys. E* **2013**, *51* (0), 60−64.
(61) Mosmann, T. Rapid Colorimetric Assay for Cellular Growth and Survival: Application to Proliferation and Cytotoxicity Assays. *J. Immunol. Methods* **1983**, *65* (1−2), 55−63.
(62) Wang, L.; Nagesha, D. K.; Selvarasah, S.; Dokmeci, M. R.; Carrier, R. L. Toxicity of Cdse Nanoparticles in Caco-2 Cell Cultures. *J. Nanobiotechnol.* **2008**, *6*, 11.
(63) Monteiro-Riviere, N. A.; Inman, A. O.; Zhang, L. W. Limitations and Relative Utility of Screening Assays to Assess Engineered Nanoparticle Toxicity in a Human Cell Line. *Toxicol. Appl. Pharmacol.* **2009**, *234* (2), 222−35.
(64) Soenen, S. J.; Montenegro, J.-M.; Abdelmonem, A. M.; Manshian, B. B.; Doak, S. H.; Parak, W. J.; De Smedt, S. C.; Braeckmans, K. The Effect of Nanoparticle Degradation on Poly-(Methacrylic Acid)-Coated Quantum Dot Toxicity: The Importance of Particle Functionality Assessment in Toxicology. *Acta Biomater.* **2014**, *10* (2), 732−741.
(65) Carneiro, P.; Fernandes, M. S.; Figueiredo, J.; Caldeira, J.; Carvalho, J.; Pinheiro, H.; Leite, M.; Melo, S.; Oliveira, P.; Simões-Correia, J.; Oliveira, M. J.; Carneiro, F.; Figueiredo, C.; Paredes, J.; Oliveira, C.; Seruca, R. E-Cadherin Dysfunction in Gastric Cancer - Cellular Consequences, Clinical Applications and Open Questions. *FEBS Lett.* **2012**, *586* (18), 2981−2989.
(66) Castillo, P. E.; Younts, T. J.; Chávez, A. E.; Hashimotodani, Y. Endocannabinoid Signaling and Synaptic Function. *Neuron* **2012**, *76* (1), 70−81.
(67) Chen, H.-C.; Chu, R. Y.; Hsu, P.-N.; Hsu, P.-I.; Lu, J.-Y.; Lai, K.-H.; Tseng, H.-H.; Chou, N.-H.; Huang, M.-S.; Tseng, C.-J.; Hsiao, M. Loss of E-Cadherin Expression Correlates with Poor Differentiation and Invasion into Adjacent Organs in Gastric Adenocarcinomas. *Cancer Lett.* **2003**, *201* (1), 97−106.
(68) Gaffuri, A. L.; Ladarre, D.; Lenkei, Z. Type-1 Cannabinoid Receptor Signaling in Neuronal Development. *Pharmacology* **2012**, *90* (1−2), 19−39.
(69) Stemmler, M. P. Cadherins in Development and Cancer. *Mol. BioSyst.* **2008**, *4* (8), 835−850.
(70) Yi, S.; Yang, Z.-l.; Miao, X.; Zou, Q.; Li, J.; Liang, L.; Zeng, G.; Chen, S. N-Cadherin and P-Cadherin Are Biomarkers for Invasion, Metastasis, and Poor Prognosis of Gallbladder Carcinomas. *Pathol., Res. Pract.* **2014**, *210* (6), 363−368.

DOI: 10.1021/acsami.5b09777
ACS Appl. Mater. Interfaces XXXX, XXX, XXX−XXX